Compact Magnetic Field Amplification by Tuned Lenz Lens

Ataollah M. A. A. S. Tajabadi, Parisa Dehghani, Dani S. Assi, Vaithinathan Karthikeyan, Chen-Bin Huang, *Senior Member, IEEE*, Hasan T. Abbas, *Senior Member, IEEE*, Vellaisamy A. L. Roy

***Abstract*—High-frequency magnetic field sensing is a vital feature of several biomedical and industrial applications. Typically, highly sensitive magnetic materials are used for such applications, yet such materials are expensive and their development is bespoke. Recently, there has been an increased interest in reshaping magnetic fields to enhance high-performance of sensing devices. In this paper, we present and evaluate the design of a Lenz lens-based miniaturised magnetic field sensor onto a single substrate. We envision that our device can be used for magnetic field-based sensing applications. Through simulations, we show that the introduction of a Lenz lens confines and enhances the magnetic field in the region of the sensor. Our design is validated using laboratory measurements that show a 40-fold improvement in the detected signal at 28.6 MHz when a Lenz lens is placed around the sensor. We also note that the enhancement leads to a 15 dB increase in the signal-to-noise ratio of the detected signal. We fabricated the design using etching techniques that are both well-known and low-cost, therefore, showing potential for mass-scale production. We demonstrate that it is not only possible to create a device that enhances magnetic field sensitivity, but also to do so in a manner that makes it easy to integrate with existing technologies. The latter feature allows it to become immediately useful for a variety of NMR applications.**

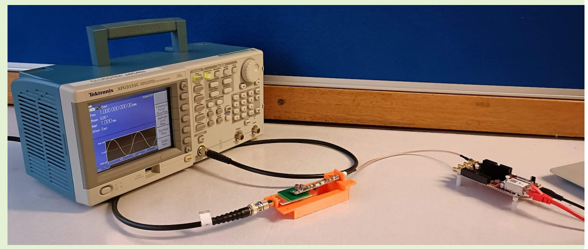

***Index Terms*—Lenz lens, magnetic fields sensing, nuclear magnetic resonance**

I. Introduction

MYRIADS of wireless technologies are currently being envisioned that will undoubtedly have a significant impact on our lives. Communication, sensing, and energy harvesting are just a few examples that have reaped benefits from the limitless potential of wireless technologies. In the realm of biomedical technologies, the detection of the magnetic field is particularly pivotal in several sensing systems. The unrelenting search for more sensitive materials and methods has led to countless developments [1]–[3]. Superconducting quantum interference devices (SQUIDs), giant magnetoresistance (GMR) sensors, tunnelling magnetoresistance (TMR) sensors, atomic magnetometers, and many more technologies have demonstrated incredible sensitivities and dynamic ranges in detecting both static and oscillating magnetic fields. There is, however, still a niche that even these technologies still struggle to satisfy and that is high-frequency magnetic field sensing. More specifically, it is the MHz to GHz frequency range of the electromagnetic spectrum where these devices don't perform as well as desired. There are many cellular, satellite, power, and quantum sensing applications that need to accurately detect high-frequency magnetic fields. The most comment method of detection is inductive coils, but devices using nanoelectromechanical systems (NEMS) [4] and giant magnetoimpedance (GMI) sensors [5] have been explored. The biggest advantages of inductive coils are that they are cheap and relatively straightforward to design; however, the trade-off is that their sensitivities are limited compared to other types of sensors. Conversely, NEMS and GMI have demonstrated incredible sensitivities, but their designs and fabrication can be quite costly. Our objective is to provide an approach that augments high-frequency magnetic sensing systems without any modification to the sensors themselves. There is an obvious benefit in pursuing materials and techniques that produce better sensors; however, this is naturally an expensive and time-consuming venture. Furthermore, the sensing area of these devices is often small, so multiple sensors would be necessary to measure an appreciable area. This problem can be significant in nuclear magnetic resonance (NMR) applications, where the sample volume greatly impacts the results. In NMR, probes are designed to fit standardized containers of predetermined dimensions, which can be problematic if the amount of sample available is not sufficient to fill a container or the sample cannot fit into a container. An alternative solution has been to create custom probes for non-standard samples, and many studies have shown them to outperform commercial probes in these situations. The main disadvantages

A. M. A. A. S. Tajabadi, P. Dehghani, D. S. Assi, V. Karthikeyan, H. T. Abbas, and V. A. L. Roy are with the James Watt School of Engineering, University of Glasgow, Glasgow G12 8QQ, U.K. (email: a.tajabadi.1@research.gla.ac.uk, p.dehghani.1@research.gla.ac.uk, d.assi.1@research.gla.ac.uk, vaithinathan.karthikeyan@glasgow.ac.uk, hasan.abbas@glasgow.ac.uk, roy.vellaisamy@glasgow.ac.uk).

C. B. Huang is with the Institute of Photonics Technologies, National Tsing Hua University, Hsinchu, Taiwan (email: robin@ee.nthu.edu.tw).

to a custom approach are that they can be difficult to construct and are specific to the sample that they were designed for. Therefore, there is a need for a sensing device that is non-sample specific, can occupy a sufficiently large area to obtain a high-quality signal, and is easy to fabricate. If we start looking at the magnetic field and what we can do with it, we quickly realize that sensing a magnetic field does not necessarily need to be a passive affair where a sensor simply sits there and waits for the signal to come to it. If one cannot improve the sensor, then their other option is to improve the field. Consider Faraday's law where a changing magnetic flux generates an electromotive force (EMF) and Lenz's law which shows this emf is directed such that it creates a magnetic flux opposing the one that created it. The question then becomes whether it is possible to have a condition where the initial magnetic flux can be amplified rather than weakened by a passive element. It is not possible by the laws of energy conservation for a given volume of space to be amplified in this manner. When describing magnetic field strength, we often refer to magnetic flux density as a metric. The ideal effect of a lens would be to augment the magnetic flux density in the region of interest while reducing the density elsewhere. Although the total magnetic flux, and therefore magnetic energy, would remain the same, its density distribution would morph to better suit the application. Essentially this is a form of localized enhancement, and also what is referred to as the 'gain' in some applications such as antenna design. This enhancement can provide a significant boost to weak signals, and consequently permit higher-resolution spectra to be produced. This is especially relevant to NMR as the signal peaks are often in the form of tuples, which can disappear in a low-resolution spectrum. Following this analogy, this gain comes at the cost of weakening the signal outside the desired region; however, for our application, this is an acceptable compromise since we know exactly where our signal is coming from. This means that the first step is to provide some form of magnetic field amplification to enhance the sensitivity of our systems. Magnetic metamaterials and metasurfaces are a class of engineered materials that produce this exact effect [6]. The interactions between individual elements can control and shape magnetic fields as desired. Increasingly, applications are looking towards these solutions as methods for expanding the capabilities of already existing systems. These ideas have been explored in the realm of wireless power transfer systems [6] and MRI systems [7]. They are fantastic solutions to this problem, but their designs are complex and require a combination of intricate calculations and detailed simulations to characterize their behaviour. The interactivity between individual unit cells is what provides their function; however, the downside to this is that all unit cells must behave in unison to maximize the system's performance. It can be a challenge to produce every unit cell exactly as desired. Furthermore, they also do not scale down well which makes them immediately unsuitable for NMR applications where space is at a premium. Another solution, that requires less difficulty to design and can be sized freely, is the Lenz lens (LL). First proposed by Schoenmaker et al. in 2013 [8], it is another method that uses induction principles to shape the magnetic field; however, it does not rely on individual units working together. The simplest design uses two concentric loops connected as shown in Fig. 1. When the initial magnetic field changes, it induces an electromotive force (EMF) in any nearby conductor, according to Faraday's law of induction. This induced EMF creates an electric current that generates its own magnetic field. The direction of the induced EMF and the resulting magnetic field is such that it opposes the change in the original magnetic field, as stated by Lenz's law. In the case of a Lenz lens, a changing magnetic field is produced by a current-carrying wire or a magnet. As the magnetic field from the wire or magnet moves through the conductive material of the lens, it induces currents that create a secondary magnetic field. The direction of this secondary magnetic field is such that it opposes the original magnetic field, creating a zone of reduced magnetic field strength. By shaping the conductive material of the lens into a specific pattern, the secondary magnetic field can be made to strengthen towards the centre of the lens and weaken towards the edges. This creates a "lens" effect that focuses the magnetic field towards a particular point or region. The behaviour of the Lenz lens is a consequence of the principles of electromagnetic induction and the interaction of magnetic fields with conductive materials. The advantage of this approach to our application is that the lens does not rely on multiple units to function and can be scaled down to the necessary size. Another significant benefit of the LL is the dampening of unwanted signals from the sample container, as well as other structural elements, due to its inherent attenuation of signals originating from regions outside the inner loop. As a result, a system with a LL would be able to use a wider range of construction materials, including polymers or other materials that are reactive to NMR experiments.

$$SNR = \frac{k_0 \frac{B_1}{i} V_{obs} N \gamma \hbar^2 I(I+1) \frac{{\omega_0}^2}{k_B T 3\sqrt{2}}}{\sqrt{4 k_B T R \Delta f}} \propto \frac{B_1}{i\sqrt{R}} \qquad (1)$$

$$F_P = \frac{{B_1}^{Peak}}{A_{obs}} \qquad (2)$$

The signal-to-noise ratio (SNR) is a metric that helps determine the resolution of an NMR system. It is a measure of the relative strength of the NMR signal to the noise in the measured spectrum. A high SNR implies that the signal is strong compared to the noise, which is desirable because it increases the accuracy and precision of the NMR measurement. The SNR equation [9] can be seen in equation 1 and involves an array of parameters. The parameter k_0 denotes a scaling factor that is utilized to account for the uniformity of the RF coil, while B_1 refers to the RF-coil's magnetic flux density. The unit current is represented by i, and the coil's sensitivity is measured as B_1 divided by i. V_{obs} stands for the observed sample volume, while the Boltzmann constant is represented by k_B. T represents the temperature of both the coil and the sample. N stands for the spin density, whereas I represents the spin quantum number. The value of Planck's constant divided by 2π is denoted by $\hbar$. ω_0, which is the Larmor frequency, is determined by the gyromagnetic ratio γ of the nucleus of interest and the strength of the static magnetic field B_0. R represents the electrical resistance of the coil, which contributes to thermal noise, and Δf stands for the bandwidth of the receiver. A second figure of merit that is especially useful in measuring the confinement and amplification capabilities of the LL is the Purcell Factor (F_P). Here we define F_P as the ratio between the peak magnetic flux density ${B_1}^{Peak}$ within a specific observation region to the area of that region A_{obs}. The Purcell Factor essentially describes how well the LL focuses the field. In this paper, we explore the LL in a novel way by integrating a magnetic field sensor into the design. Previous studies have leveraged the LL as an interface between the sample and a sensing element that was larger than both the LL and the sample. The paper by Jouda et al. [10] revealed that a smaller transceiver placed closer to the sample outperforms a larger transceiver combined with a LL. Here, we propose a new configuration that takes full advantage of the lens by integrating the magnetic field sensor into its centre. Additionally, the miniaturization of the LL and receiver aims to increase the F_P of the coils, thus enhancing the SNR of the system. The main objectives are to first demonstrate the effectiveness of the LL as an amplifier for our application and secondly to develop a less complex method of designing microprobes that leverages existing low-cost fabrication processes.

II. Methods

A. Lenz Lens Design and Simulation

We first began by choosing what type of magnetic sensor we wanted to use. We intend to use the Lenz lens and magnetic sensor as the receiver element in our NMR experiments, so henceforth we will refer to this device as the receiver board. The transmitting element will be known as the transmitter board. As previously mentioned, the inductive coil requires the least time and cost to fabricate, so we chose it as our sensor. In the future, we will revisit these experiments with NEMS or GMI sensors. An inductive coil's geometry can be either volumetric or planar. We designed a planar coil that can be easily complemented with a planar lens. The advantage of using two planar geometries is that they can be integrated onto a single flat substrate, which simplifies the fabrication. Our constraints in the receiver board design were mainly dictated by the size of our main magnet and the fabrication process. The magnet we used for NMR experiments was the NMR7014-066 (Xiamen Dexing Magnet Tech. Co. Ltd, China) and it had a gap of 14 mm between the poles. The receiver board design and dimensions are shown in Fig. 1. The width of the square substrate W_s was set at 12 mm to leave enough space between the edges of the board and poles. We then chose the outer LL diameter D_{LLO} to be 10 mm to provide enough space between the edge of the substrate and the LL. When designing the LL, the ratio of the outer to inner ring diameters is a key parameter as it determines the trade-off between amplification amount and area [9]. The inner LL diameter D_{LLI} was a balance between maximizing the amplification while keeping the limits of the fabrication process in mind since we also needed to have a receiver coil sit within the inner loop. The smallest receiver coil that we could produce had a diameter D_{RC} to 2.9 mm, and consequently, D_{LLI} was 5 mm. The gaps W_{LLG} and W_{RCG} were set to 1 and 0.5 mm. Finally, the trace widths of the LL T_{LL} and receiver coil T_{RC} were set to 1.0 mm and 0.7 mm respectively. The transmitter coil represents the NMR sample and was placed in the same position as the NMR sample would be in the future. Specifically, it was placed directly in front of the receiver board with a spacing of 1 mm. The 1 mm gap reflects the thickness of the NMR sample container's walls.

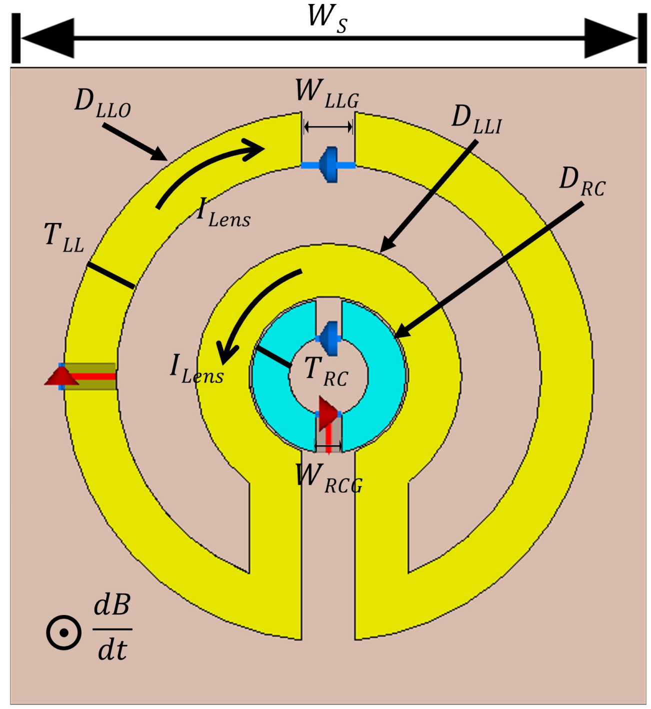

Fig. 1: Design of the receiver coil (blue) and Lens lens (yellow) on the substrate (grey). The blue arrows represent the lumped elements while the red arrows represent lumped ports.

Since both the LL and coil are inductors, their impedances increase proportionally to the frequency. In the MHz and GHz regimes, this can correspond to a high reactance that generates non-linearities in the signal and deteriorates its quality. Therefore, there is a need to reduce or eliminate any undesired reactances as much as possible. To accomplish that, we designed both the LL and coil to be paired with an appropriate capacitor in an LC tank configuration [11]. The resonant behavior of the system leads to a narrowband frequency operation range; however, this is an acceptable compromise for our current study as we will only be performing proton NMR. This feature is reflected in the designs with a gap where the capacitor would be connected across. Simulations were performed using the frequency domain solver of CST Studio Suite 2019 (Dassault Systèmes SE, France) [12] to quantify and visualize the behaviour of the proposed design. We ran the simulation on a personal computer with a system with 11th Gen Intel® Core ™ i7-1185G7 and 16 GB of RAM. Our signal source was modelled using a coil with an outer diameter equal to D_{LLO} and trace thickness equal to T_{LL}. D_{LLO} was chosen to equal the diameter of the sample container that we planned to use during our NMR experiments and the trace thickness was chosen to minimize parasitic resistance. The distance between the source coil and the receiver coil was set to 1 mm. The capacitors were modelled using lumped elements placed across the gaps we designed. Discrete face ports of the S-parameter type are placed on the transmitter and receiver coils.

B. Circuit Design

The next step was to fabricate the design. We placed all the components on a single board, including the capacitors and other necessary accessories. Two additional considerations needed to be made at this stage. Firstly, we had to match the receiver coil's impedance to that of the measuring equipment of 50 Ω, since the receiver coil did not inherently possess a 50 Ω impedance. There are various matching topologies that can be used, and we chose the π-match network for its natural ability to filter out any higher-order harmonics that could distort our signal. The network transformed the 50 Ω source impedance to a 2 Ω. The load impedance was chosen by considering the total resistance of the receiver coil and components, and then selecting a resistance that was significantly higher than the sum of those values. This provided a load impedance that was large enough not to be affected by the circuit's parasitics, including any additional parasitics generated by the traces, while remaining small enough as to minimize the thermal noise. Equation 3 describes the relationship between the elements of a π network. The Z_{input} is the impedance of the matching circuit as a whole and the $R_L + jX_L$ defines the load impedance. C_S, C_L, and L are the source capacitor, load capacitor, and inductor respectively.

$$Z_{input} = \left[\left((R_L + jX_L) \parallel \left(\frac{1}{jw \cdot C_L} \right) \right) + jw \cdot L \right] \parallel \left(\frac{1}{jw \cdot C_S} \right) \quad (3)$$

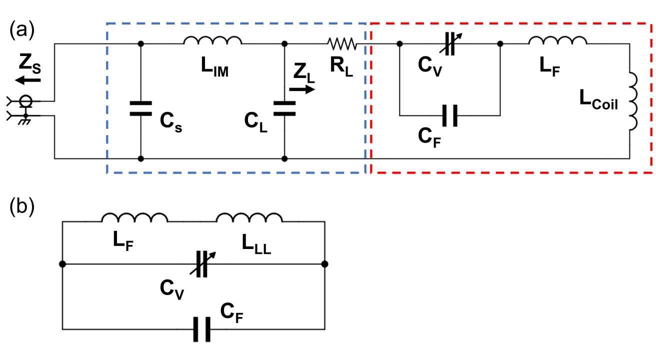

Fig. 2: The top side of the board with Lenz lens and receiver coil before components were added.

The second consideration was the receiver coil's inductance as it was key to calculating the capacitance of the LC tank. Estimating the inductance using an inductor design software Coil64 [13] gave us a value in the order of a few nH. The issue here is that the stray inductances created by traces and circuit components are of a similar order to the receiver coil's inductance, and thus can shift the total inductance. This could significantly impact the resonant behaviour of the system. To avoid this issue, we added a fixed-value inductor into the LC tank with a value that was two orders of magnitude higher than that of our receiver coil and connecting traces. Finally, we needed a capacitor that had a reactance equal to and opposite to that of our inductor at the required frequency to achieve resonance. Using this condition, we can calculate the capacitance required. Again, considerations of the parasitic capacitances must be done to ensure that the resonant capacitor's value is not significantly impacted either. To account for any shifts that arose from this effect, and also to allow for a finely tuned LC tank, we added a variable capacitor in parallel to a fixed-value capacitor. This way gives a method of manually setting the value of the capacitor. The LL LC tank circuit was designed the same way. The circuit schematic of the LL and receiver coil can be seen in Fig. 2. The values of the receiver board components can be seen in I.

TABLE I: Table of receiver board component values.

Rx Coil Impedance	L_{Coil}	3 nH
Fixed Impedance	L_F	150 nH
Variable Capacitance	C_V	2x 50 pF
Fixed Capacitance	C_F	150 pF
Load Resistance	R_L	2 Ω
Load Capacitance	C_L	5560 pF
Pi Network Inductance	L_{IM}	30 nH
Source Capacitance	C_S	1240 pF

(a) (b)

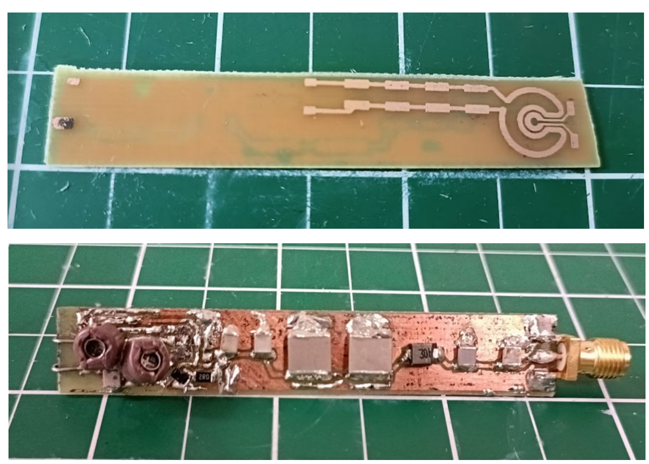

Fig. 3: Top: The top side of the board with Lenz lens and receiver coil before components were added. Bottom: Bottom side of the receiver board with components.

C. Fabrication

The board was fabricated using an in-house wet etching process on a double-sided FR-4 copper clad, with a copper thickness of 35 μm and a substrate thickness of 0.8 mm. The fabricated LL and assembled board can be seen in Fig. 3(a) and (b) respectively. The board was made using the following

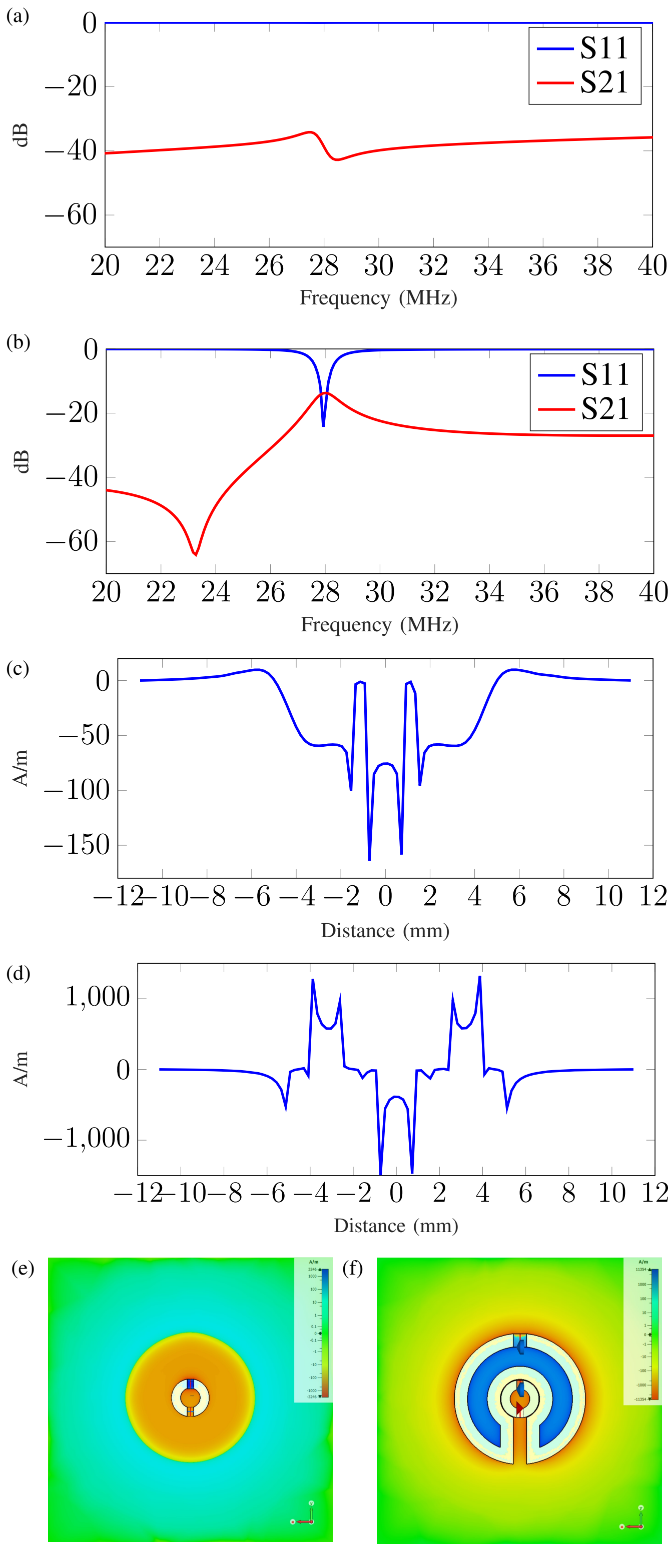

Fig. 4: Simulation results from designs without (a), (c), (e), and with the Lenz lens (b), (d), (f). (a) & (b) S-parameter results from simulation with a distinct peak at 28.6 MHz. (c) & (d) Z-axis magnetic field strength along the red dotted line as shown in the inset. (e) 2D magnetic field strength at the surface of the receiver.

steps. The first step was to clean the blank copper-clad board using acetone and an abrasive pad to remove any undesired elements that could compromise the mask transfer process. In the second step, we printed our mask onto photo paper using a laser printer and applied a few drops of a solution made from 3 parts acetone mixed with 8 parts ethanol by volume. After applying pressure over a duration of 90 seconds, the board was then placed into a water bath and left for 5 minutes to ensure the transfer process had stopped. Once the mask was successfully transferred, the third step was to etch the board in a solution of ferric chloride until the exposed copper had dissolved. The board was then transferred to a water bath for 5 minutes and the final step was to remove the mask using acetone. Once the board was fabricated, the individual components were soldered onto it to form the tuning circuit for the LL, as well as the tuning circuit and impedance matching circuit for the receiver coil.

III. Results and Discussion

A. Simulation Results

To analyse the proposed design, we investigated the frequency domain scattering parameters of the LL. In particular, we investigated the S_{21} scattering parameter to study the effect of the lens. All designs were aimed to operate at 28.6 MHz as our Larmour frequency for proton NMR [14]. Figure 4 shows the impact of introducing a LL around the receiver coil. As shown in Figs. 4(a) and (b), the corresponding S_{21} parameter values obtained with and without the LL around the coil were -14.873 dB and -33.874 dB, respectively. Observing the S_{11} shows that almost all the input power is reflected back to the source when there is no lens in the system (4 a), which indicates that the receivers coil's performance is significantly impacted by the addition of the LL. The behavior of the magnetic field component which is normal to the receiver coil plane (H_z) can be seen in Figs. 4(c)-(f). By comparing the one-dimensional field plots of Figs. 4(c)-(d), we can note the magnetic field enhancement by a factor of 9.09 in the focusing region where the coil is placed. Inside the area of the receiver coil the H_z along the diameter of the receiver coil in the x-axis peaks at around -165 A/m in control and -1500 A/m in the LL simulations, with values of -75.6 A/m and -387.64 A/m in their centres respectively. Moreover, it can also be observed that with the introduction of the LL, the magnetic field decays sharply as we move away from the centre. The two-dimensional plots of the magnetic field are shown in Figs. 4(e) and (f) from which it is clear, that a field hotspot is created inside the receiver coil after the LL is introduced. Calculating the magnetic flux density from the results of the LL simulation gives us a value of 0.485 mT. Comparing that to the results of Schoenmaker et al. [8] and Spengler et al. [9], we see an improvement of approximately 4.8 and 2.4 times in absolute magnetic flux density. Calculating F_P gives us a value of 9.55 and 1.064 T/m^2 for Spengler et al. and our designs respectively. Although our study deploys the LL in conditions that are different to those in the aforementioned studies, our simulation results further demonstrate the strength and versatility of this method.

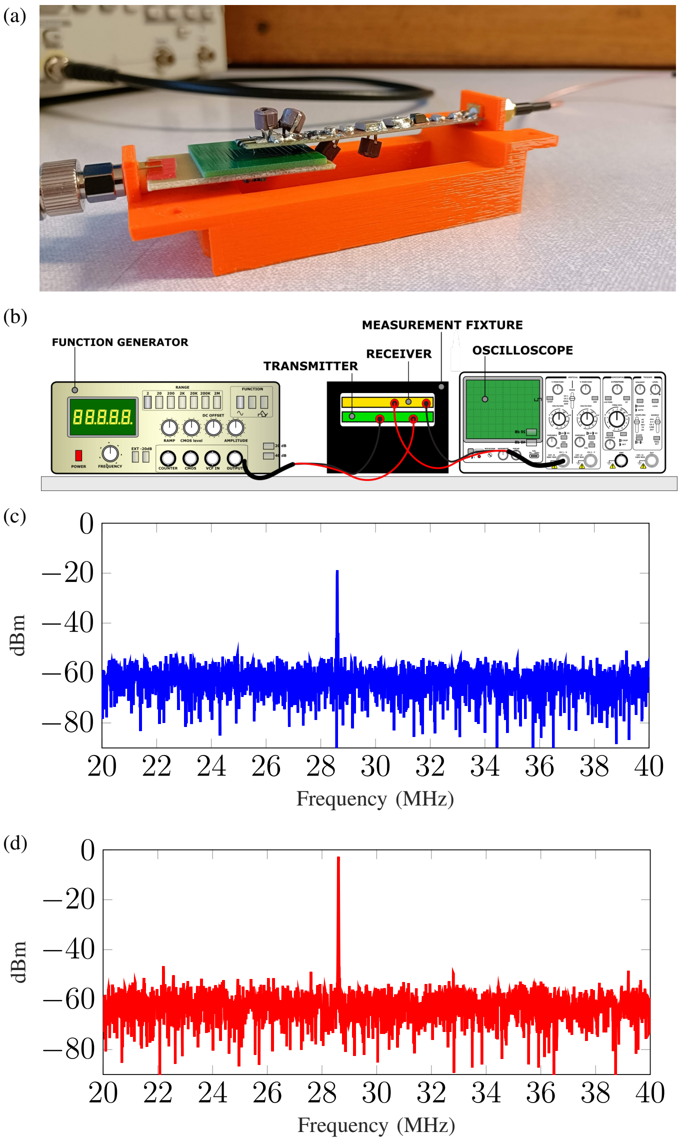

Fig. 5: (a) & (b) Experimental setup used where the receiver board is placed over the transmitter board. (c) & (d) Power spectrum recorded by the oscilloscope for experiments with (red) and without (blue) the Lenz lens.

B. Measurement

Once the board was prepared, we created an experimental setup [Fig. 5 (a)] to test its effectiveness. The experiment measured the power transferred from the transmitter to the receiver. This allowed us to test whether the board responds at the expected frequency and if its signal-to-noise ratio is high enough to be an effective method of amplifying magnetic fields. The latter is especially important as the LL will not be an effective solution if it introduces significant noise into the signal. To ensure our results were consistent, we 3D printed a holder which kept the boards at a fixed position relative to each other. SMA cables then connected the transmitter to an AFG3151C (Tektronix inc., United States) signal generator that created a continuous sinusoidal wave of 2 W at 28.6 MHz and the receiver to a STEMlab 125-10 (Red Pitaya d.o.o, Slovenia) microcontroller that acted as the oscilloscope with a discreet Fourier transform (DFT) functionality. The transmitted signal was seen as a peak on the oscilloscope when using the DFT function. Fig. 4 (b) and (c) show the power spectrum of experiments without and with the LL, respectively. In both experiments, we can see a clear peak at the expected frequency of 28.6 MHz. The power detected with the LL present was -2.770 dBm or 0.528 mW. However, when the LL is absent it was -18.854 dBm or 0.0130 mW. The presence of the LL amplified the received signal by over 40 times.

IV. Conclusion

The success of future nuclear magnetic resonance (NMR) sensors and probes is going to be governed by the sensitivity and portability of the devices. Furthermore, it is equally important that the said devices can be easily integrated with existing technologies. In this work, we presented and evaluated a low-cost and standalone Lenz lens (LL)-based receiver coil that can be used as a highly sensitive NMR sensor for biomarker applications. The addition of a LL demonstrated an 18.91 dB in the S_{21} parameters at the resonant frequency of 28.6 MHz. Furthermore, the sensitivity of the system is also improved as the magnetic field strength around the receiver coil is enhanced by a factor of 9. We aim to deploy this system for biomarker detection in urine samples; however, we envision it to be suitable for a whole host of liquid NMR applications in both open- and closed-magnet configurations.

Acknowledgment

We would like to thank Dr Steven Neale for graciously lending his equipment and lab for this project and the University of Glasgow for their support.

References

[1] M. A. Khan, J. Sun, B. Li, A. Przybysz, and J. Kosel, "Magnetic sensors-A review and recent technologies," Eng. Res. Express, vol. 3, no. 2, p. 022005, Jun. 2021, doi: 10.1088/2631-8695/ac0838.

[2] N. Alberto, M. F. Domingues, C. Marques, P. André, and P. Antunes, "Optical Fiber Magnetic Field Sensors Based on Magnetic Fluid: A Review," Sensors, vol. 18, no. 12, Art. no. 12, Dec. 2018, doi: 10.3390/s18124325.

[3] D. Murzin et al., "Ultrasensitive Magnetic Field Sensors for Biomedical Applications," Sensors, vol. 20, no. 6, Art. no. 6, Jan. 2020, doi: 10.3390/s20061569.

[4] M. Zaeimbashi et al., "Ultra-compact dual-band smart NEMS magnetoelectric antennas for simultaneous wireless energy harvesting and magnetic field sensing," Nat Commun, vol. 12, no. 1, Art. no. 1, May 2021, doi: 10.1038/s41467-021-23256-z.

[5] O. Thiabgoh, T. Eggers, V. O. Jimenez, S. D. Jiang, J. F. Sun, and M. H. Phan, "Real-time monitoring of position and motion of a non-stationary object with a highly sensitive magnetic impedance sensor," Journal of Science: Advanced Materials and Devices, vol. 3, no. 1, pp. 122–128, Mar. 2018, doi: 10.1016/j.jsamd.2018.01.006.

[6] K. Sun et al., "An overview of metamaterials and their achievements in wireless power transfer," J. Mater. Chem. C, vol. 6, no. 12, pp. 2925–2943, 2018, doi: 10.1039/C7TC03384B.

[7] M. J. Freire, R. Marques, and L. Jelinek, "Experimental demonstration of a $\mu{=}{-}1$ metamaterial lens for magnetic resonance imaging," Appl. Phys. Lett., vol. 93, no. 23, p. 231108, Dec. 2008, doi: 10.1063/1.3043725.

[8] J. Schoenmaker, K. R. Pirota, and J. C. Teixeira, "Magnetic flux amplification by Lenz lenses," Review of Scientific Instruments, vol. 84, no. 8, p. 085120, Aug. 2013, doi: 10.1063/1.4819234.

[9] N. Spengler, P. T. While, M. V. Meissner, U. Wallrabe, and J. G. Korvink, "Magnetic Lenz lenses improve the limit-of-detection in nuclear magnetic resonance," PLOS ONE, vol. 12, no. 8, p. e0182779, Aug. 2017, doi: 10.1371/journal.pone.0182779.
[10] M. Jouda et al., "A comparison of Lenz lenses and LC resonators for NMR signal enhancement," Concepts in Magnetic Resonance Part B: Magnetic Resonance Engineering, vol. 47B, no. 3, p. e21357, 2017, doi: 10.1002/cmr.b.21357.
[11] R. Kamberger et al., "Improved method for MR microscopy of brain tissue cultured with the interface method combined with Lenz lenses," Magnetic Resonance Imaging, vol. 52, pp. 24–32, Oct. 2018, doi: 10.1016/j.mri.2018.05.010.
[12] "CST Studio Suite & Opera Recommended Hardware." https://www.3ds.com/support/hardware-and-software/simulia-system-information/cst-studio-suite-opera/cst-studio-suite/ (accessed Dec. 20, 2022).
[13] "Coil32 - Coil64 for 64-bit Windows - Coil64 for 64-bit Windows." https://coil32.net/download-coil64-for-windows.html (accessed Dec. 20, 2022).
[14] "CODATA Value: proton gyromagnetic ratio in MHz/T." https://physics.nist.gov/cgi-bin/cuu/Value?gammapbar (accessed Feb. 01, 2023).

Ataollah M. A. A. S. Tajabadi received his B.Eng in Biomedical Engineering from King's College London, London, U.K., and his M.Res in Medical Robotics and Image-Guided Intervention from Imperial College London, London, U.K. He is currently working towards a PhD at the University of Glasgow, Glasgow, U.K. His research focuses on Nuclear Magnetic Resonance technology for medical applications.

Parisa Dehghani awarded her master's degree from Isfahan University in field of Nanobiotechnology and bachelor's degree from Shiraz University, Iran. Her main research interest is Biosensors. She starts her PhD on developing Bio-FET sensors at the University of Glasgow, United Kingdom, from October 2020. She is author/co-author of 5 journal articles and one book chapter of "Neural Regenerative Nanomedicine" book by the Elsevier. She has presentations in 10 conferences and workshops.

Dani S. Assi is a Biomedical Engineer with a BS degree from the Technical University of Lodz (TUL) and an MS degree from the University of Glasgow (UofG). He is currently pursuing a Ph.D. at the University of Glasgow, where his research focuses on the development of neuromorphic synaptic devices for next-generation computation. Dani is deeply passionate about the convergence of engineering, biology, material science, and computer science, where he is dedicated to developing innovative technologies capable of emulating the intricate operations of the brain, thereby pushing the frontiers of computational neuroscience to new heights.

Vaithinathan Karthikeyan is presently a postdoc at James Watt School of Engineering at the University of Glasgow. He did his PhD in Materials Engineering at the City University of Hong Kong. His research focuses on interdisciplinary research areas of materials science for energy harvesting devices, biosensors, neuromorphic electronics and terahertz electronics. He has published over 30 articles in journals such as Nature Communications, Advanced Science.

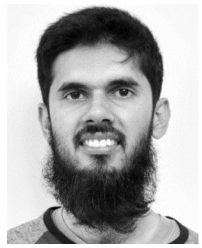

Hasan T. Abbas received the B.Sc. degree (with Hons.) in electrical engineering from the University of Engineering and Technology (UET), Lahore, Pakistan, and the PhD degree in electrical and computer engineering from Texas A&M University, College Station, TX, USA, in 2017. From 2009 to 2012, he was a Junior Lecturer with the Department of Electrical Engineering, KSK campus, UET Lahore. From April 2018 to June 2019, he was a Postdoctoral Research Associate with the Department of Electrical and Computer Engineering, at Texas A&M University at Qatar, Doha, Qatar. Since June 2019, he has been a Lecturer with the James Watt School of Engineering, University of Glasgow, Glasgow, U.K. His research interests include plasmonics, terahertz sensing, and developing numerical methods in electromagnetics. He was the recipient of the prestigious Fulbright Scholarship.

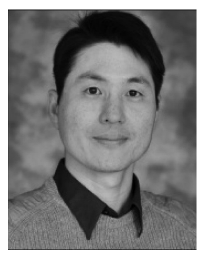

Chen-Bin Huang (M'99–SM'04) received the B.S. degree in electrical engineering from National Tsing Hua University, Hsinchu, Taiwan, in 1997, the M.S. degree in electro-optical engineering from National Chiao Tung University, Hsinchu, in 1999, and the Ph.D. degree from the School of Electrical and Computer Engineering, Purdue University, West Lafayette, IN, USA, in 2008. He has worked at Bell Laboratories (Alcatel-Lucent) in the USA and the Opto-Electronics and Systems Laboratories of the Industrial Technology Research Institute (ITRI) in Taiwan. He has worked as a Visiting Scientist at the Physics Institute, University of Würzburg, Würzburg, Germany, and the Materials Research Institute, Northwestern University, Evanston, IL, USA. He joined the Institute of Photonics Technologies, National Tsing-Hua University, as an Assistant Professor in 2008 and was promoted to Associate Professor in 2012. His current research interests include optical and millimeter-wave arbitrary waveform generations, nanoplasmonics, and applications of optical frequency combs. He has authored/coauthored one book chapter and more than 100 journal and conference papers. He is a holder of seven USA patents and 13 Taiwan patents.

Vellaisamy A. L. Roy is a Professor of Intelligent systems at the James Watt School of Engineering, University of Glasgow. He works on multidisciplinary research blending device physics with materials chemistry and electronic engineering. He has published over 200 articles in journals such as Nature Communications, Advanced Materials, Advanced Functional Materials, Analytical Chemistry etc. In addition, he has 21 US/International/Chinese patents. He received a gold medal for his "Sensor Platform" at the International Exhibition of Inventions Geneva 2019.